**ORIGINAL ARTICLE**

# Investigation of tool wear and energy consumption in machining Ti6Al4V alloy with uncoated tools

Muhammad Younas[1] · Mushtaq Khan[2] · Syed Husain Imran Jaffery[3] · Zarak Khan[5] · Nawar Khan[4]

## Abstract

This research studies the energy consumption and wear mechanism of carbide cutting tools in dry machining of Ti6Al4V alloy. In the first phase of experiments, full factorial design experiments were employed to study the tool wear rate ($R$) and specific cutting energy (SCE) with respect to the machining conditions (cutting speed and feed rate). Results showed that machining responses such as tool wear and energy consumption are affected by cutting conditions, thus requiring investigation to understand the wear mechanisms. Therefore, in the second phase, additional experiments were performed to investigate the tool-workpiece interactions at the cutting conditions reported to have low, moderate, and high tool wear. It was revealed that strong adhesion and material transfer between the tool and workpiece caused high wear. Electron dispersive X-ray spectroscopy (EDX) analysis of worn tools showed that the transfer of tungsten (W) and cobalt (Co) to the workpiece and titanium to the tool surface is the primary cause of tool deterioration. As a result, diffusion and dissolution have degraded cutting performance and weakened the tool edge, leading to rapid wear. Furthermore, worn tools resulted in relatively higher energy consumption per unit volume of material removed at the tooltip. The degradation of cutting performance and weakening of the tool edge results in rapid wear and higher energy consumption. The study suggests that minimizing tool wear is crucial for energy reduction, improved sustainability, and cleaner production goals in dry machining of titanium-based alloys.

**Keywords** Energy consumption · Tool wear · Titanium alloys · Wear mechanisms · Dry machining

## Abbreviations

| | |
|---|---|
| $P_{act}$ | Actual cut power |
| $P_{air}$ | Air cut power |
| $r$ | Chip compression ratio |
| $h_2$ | Chip thickness after the cut |
| CNC | Computer numerical control |
| $V$ | Cutting speed |
| $d$ | Depth of cut |
| EDX | Energy dispersive X-ray |
| $f$ | Feed rate |
| $VB$ | Flank wear |
| MRR | Material removal rate |
| NC | Numerical control |
| rpm | Revolutions per minute |
| SEM | Scanning electron microscopy |
| SCE | Specific cutting energy |
| $h_1$ | Undeformed chip thickness |
| $R$ | Wear rate parameter |

✉ Muhammad Younas
  m.younas@rgu.ac.uk

  Mushtaq Khan
  mkhan7@pmu.edu.sa

  Syed Husain Imran Jaffery
  imran@smme.edu.pk

  Zarak Khan
  zarak.khan@hitecuni.edu.pk

  Nawar Khan
  nawar.khan@riphah.edu.pk

1 School of Engineering, Robert Gordon University, N447 Sir Ian Wood Building, Aberdeen AB10 7QB, UK

2 Mechanical Engineering Department, Prince Mohammad Bin Fahd University, 31952 Al-Khobar, Saudi Arabia

3 National University of Sciences and Technology, Sector H-12, Islamabad 44000, Pakistan

4 Riphah International University, Islamabad, Pakistan

5 Department of Mechanical Engineering, HITEC University, Taxila, Pakistan

# 1 Introduction

Modern manufacturing industries are striving to reduce costs, improve part quality, and minimize the environmental impact of their processes, including the use of eco-friendly cutting fluids. Achieving long-term production goals and improving machining performance metrics, such as tool wear, tool life, and part quality, are critical to meeting these objectives [1]. However, energy consumption in machining processes requires special attention since operators may use carbon-intensive operational parameters. Machining titanium alloys is particularly challenging due to their difficult nature, including high strength-to-density ratios, corrosion resistance, chemical reactivity, and high hot hardness [2]. These properties make titanium alloys preferred in medical, aerospace, and offshore applications. Among titanium alloys, TiAl4V is the most commonly produced (α+β) alloy, accounting for half of the produced tonnage. Various grades of uncoated carbide are typically used to cut these alloys, but improving their machinability remains a key challenge for both industries and researchers. This requires the use of modern tooling and effective process parameters to mitigate the impact of machining parameters on critical machining responses.

Machining is a critical requirement in most production industries, including aerospace, automotive, and biomedical, due to the need for complex, high-quality parts. Despite the wide use of turning and milling processes, there is still a need to improve the quality and accuracy of the parts as a part of constant process improvement. As a result, most of the recent researchers have focused on improving the cutting process, including the type of tools used [3], increasing production rates, and developing new methods and strategies for high-speed machining under dry, wet, and cryogenic conditions [4]. About 25% of the global energy consumption accounts for the industrial sector with the machining processes a potential contributor in manufacturing settings [5]. The industrial sector energy consumption in the UK that includes manufacturing, construction, and mining is estimated to be 17% of the final total energy consumed. This shows a huge potential for energy savings in the manufacturing sector [6, 7]. Manufacturing energy use accounts for a large component of the UK's greenhouse gas emissions, accounting for roughly 10%. It is therefore crucial to reduce energy consumption in industrial processes to help achieve the country's carbon reduction targets. To address this, recent research has focused on improving machining performance through better tool materials, increased productivity, and eco-friendly technologies to achieve greener, healthier, and safer operations [8]. Many parameters, such as dry and minimum quantity of lubricant (MQL) machining, nanofluids, biodegradable vegetable oils, and cryogenic lubrication, enhance part quality and improve machining performance while reducing environmental damage and production costs.

Dry machining is an effective method for achieving cleaner production goals and reducing the harmful effects of cutting fluids [9]. However, the tool chip interface in dry machining experiences high temperatures and complex interactions, resulting in accelerated tool wear. The heat and friction at the interface become even more complex and intensive when cutting titanium-based alloys at high cutting speeds. Previous studies have focused on wear phenomena in machining Ti6Al4V alloys and reported that WC-Co tools show better hardness, wear resistance, and chemical inertness, making them widely used in machining titanium alloys [10]. Therefore, an uncoated carbide tool was used in this study.

Tool wear is critical in controlling other properties when machining titanium alloys. Previous studies have demonstrated that wear can impact energy consumption and



**Fig. 1** Machining setup for turning experiments
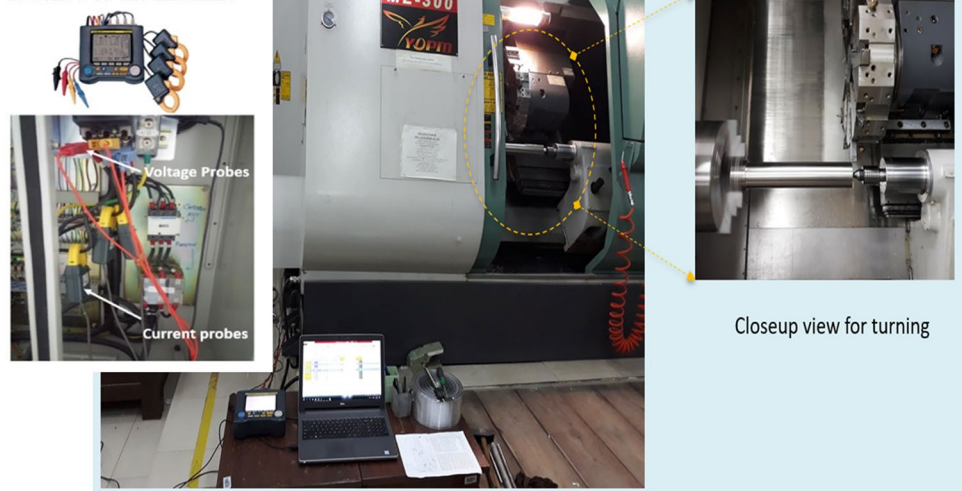
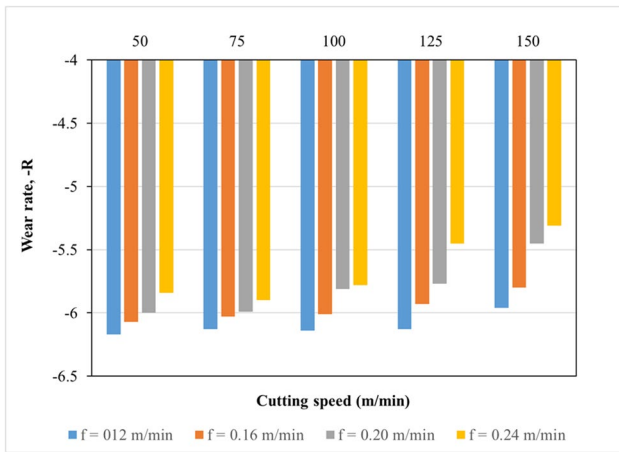**Fig. 2** Tool wear with respect to the cutting conditions
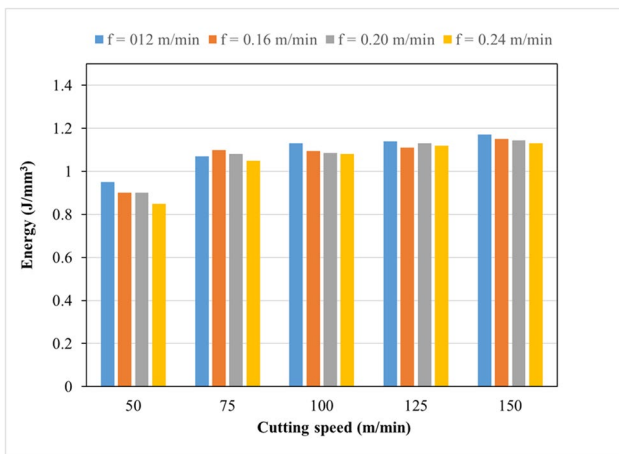


**Fig. 3** SCE with respect to the cutting conditions
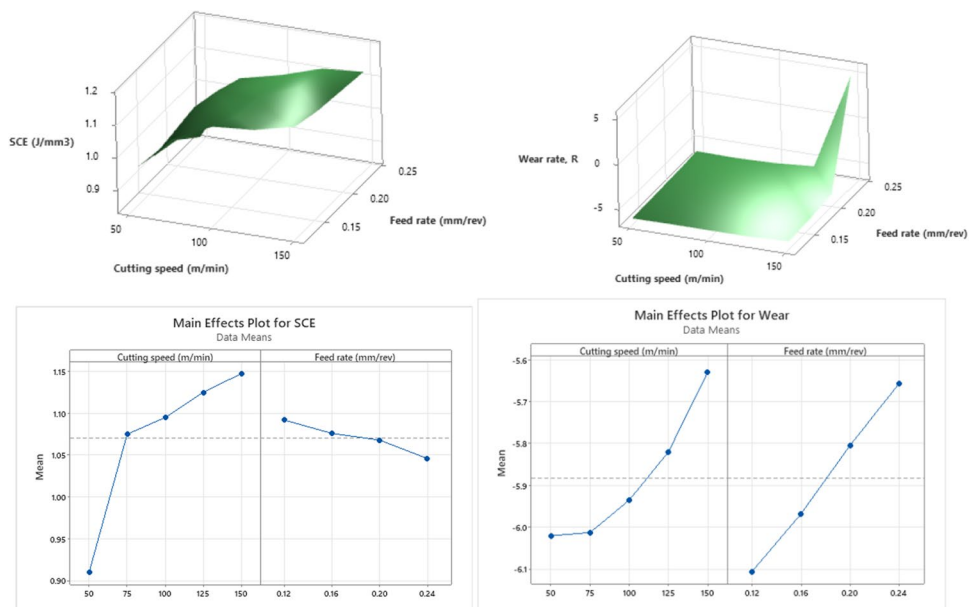
identified it as a possible way to control other machining characteristics [11, 12]. Common wear morphologies reported in titanium machining using uncoated tools include crater and flank wear well as tool chipping and plastic damage [13]. To improve the shop floor machining environment in terms of part quality, production cost, and cutting energy used in the process, wear mechanism analysis is critical. While most studies have discussed the types and nature of wear mechanisms that can occur when cutting a variety of materials, including aluminum, steel, and titanium alloys, it has been widely reported that the latter has a high reactivity with the tool material [14–16]. Diffusion and dissolution are the primary sources of tool wear when machining titanium-based alloys, and some authors suggest a combination of adhesion, attrition, and diffusion wear [17]. Others have proposed that at higher cutting condition, an attrition wear mechanism controls the flank and rake crater, while a diffusion wear mechanism controls them at medium-to-high cutting rates. [18]. Diffusion and chemical wear are also considered the main causes of deterioration when machining titanium alloy with a cemented carbide tool. Carbon diffusion causes worn flank and rake regions, and titanium reacts with carbide to generate TiC, which has a strong deformation strength and can be applied as a tool protection layer [16]. Several papers have also discussed the application of scanning electron microscopy (SEM) in combination with X-ray energy-dispersive spectrometry (XEDS) to examine the as-worn tools.

Achieving sustainability in machining processes involves improving process characteristics such as tool wear, roughness, cutting forces, and energy efficiency. Machine tools have been identified as the primary energy consumer in manufacturing environments, making it crucial to study tool wear mechanisms in titanium alloy machining to understand

**Fig. 4** Surface plots and main effect plots for tool wear and SCE

**Fig. 5** Additional cutting conditions selected for turning Ti6Al4V [19]
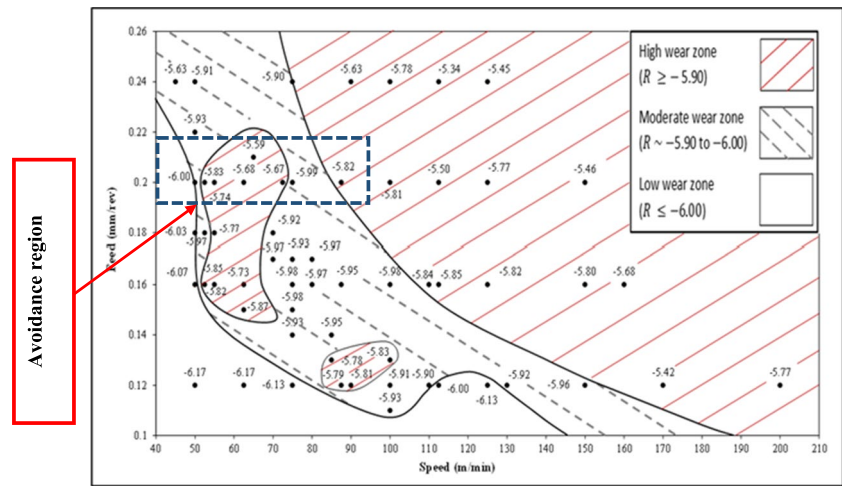


energy consumption [19, 20]. The effect of tool vibration and force signal is another important factor to consider during machining, particularly for hard-to-cut materials. Numerical and experimental results were reported to optimize process parameters for reduced power consumption, cutter vibration, and forces [21], and thus methodologies were also proposed for tool vibration-based wear and surface roughness estimation [22]. Improving machining performance and understanding the complexity of the interaction at the tooltip requires a comprehensive investigation of wear mechanisms. Thus, this research aims to investigate the effect of cutting conditions on tool wear and energy consumption and analyzes the tool wear mechanisms in uncoated tools after turning Ti6AL4V alloy using SEM/EDX and to correlate tool wear with process energy consumption. Analysis of the tools with SEM/EDX enables visualization and distribution of reaction products of the flank wear region occurring at different cutting speeds for dry machining titanium using uncoated tools. Furthermore, high tool wear cutting conditions were identified, and tool wear, specific cutting energy, and chip characteristics were evaluated. The study is significant for achieving improved tool life and energy consumption in the dry machining of titanium-based alloys using uncoated carbide tools.

## 1.1 Research motivation

This study builds upon a previous investigation focused on developing wear and energy maps, characterizing cutting conditions in regions of high, low, and moderate wear and

energy [19]. The current study explores a deeper understanding of wear phenomena by investigating the interaction between the tool and workpiece. It specifically examines the transfer of elements between the tool and workpiece and its impact on energy consumption. Understanding the tool work interaction under a dry-cutting environment will lead to a better understanding of the materials transfer for tool materials selection and possible tool coatings development. The result of this study is valuable for optimizing dry-cutting parameters, leading to potential benefits in tool

**Table 1** Analysis of the chemical composition of Ti-6Al-4V (weight %)

| Ti | V | Al | Fe | Cu | Cr |
|---|---|---|---|---|---|
| 89.44 | 4.2 | 5.7 | 0.15 | 0.003 | 0.0023 |

**Table 2** Full factorial experiments for wear and energy analysis

| Sr. # | Cutting speed (m/min) | Feed rate (mm/rev) |
|---|---|---|
| 1 | 50 | 0.12 |
| 2 | 50 | 0.16 |
| 3 | 50 | 0.2 |
| 4 | 50 | 0.24 |
| 5 | 75 | 0.12 |
| 6 | 75 | 0.16 |
| 7 | 75 | 0.2 |
| 8 | 75 | 0.24 |
| 9 | 100 | 0.12 |
| 10 | 100 | 0.16 |
| 11 | 100 | 0.2 |
| 12 | 100 | 0.24 |
| 13 | 125 | 0.12 |
| 14 | 125 | 0.16 |
| 15 | 125 | 0.2 |
| 16 | 125 | 0.24 |
| 17 | 150 | 0.12 |
| 18 | 150 | 0.16 |
| 19 | 150 | 0.2 |
| 20 | 150 | 0.24 |

**Table 3** Tool wear and SCE values obtained from the experiments

| Sr. # | Cutting speed (m/min) | Feed rate (mm/rev) | Wear rate, R | SCE (J/mm$^3$) |
|-------|----------------------|--------------------|--------------|----------------|
| 1 | 50 | 0.12 | −6.17 | 0.95 |
| 2 | 50 | 0.16 | −6.07 | 0.93 |
| 3 | 50 | 0.2 | −6.00 | 0.91 |
| 4 | 50 | 0.24 | −5.84 | 0.85 |
| 5 | 75 | 0.12 | −6.13 | 1.07 |
| 6 | 75 | 0.16 | −6.03 | 1.10 |
| 7 | 75 | 0.2 | −5.99 | 1.08 |
| 8 | 75 | 0.24 | −5.9 | 1.05 |
| 9 | 100 | 0.12 | −6.14 | 1.13 |
| 10 | 100 | 0.16 | −6.01 | 1.09 |
| 11 | 100 | 0.2 | −5.81 | 1.08 |
| 12 | 100 | 0.24 | −5.78 | 1.08 |
| 13 | 125 | 0.12 | −6.13 | 1.14 |
| 14 | 125 | 0.16 | −5.93 | 1.11 |
| 15 | 125 | 0.2 | −5.77 | 1.13 |
| 16 | 125 | 0.24 | −5.45 | 1.12 |
| 17 | 150 | 0.12 | −5.96 | 1.17 |
| 18 | 150 | 0.16 | −5.8 | 1.15 |
| 19 | 150 | 0.2 | −5.45 | 1.14 |
| 20 | 150 | 0.24 | −5.31 | 1.13 |

cost reduction and energy consumption, especially in the machining of titanium-based alloys.

## 2 Experimental section

The study involved conducting turning experiments on solid bars of Ti6Al4V alloy using uncoated H13-grade carbide inserts. The chemical composition of the workpiece alloy used for turning tests is presented in Table 1. A full factorial design of experiments (Table 2) was employed for turning experiments selected from the range of cutting parameters recommended by the tool manufacturer. All experiments were conducted at a constant depth of cut of 1 mm.Experiments were performed under dry conditions as it allows to explore the inherent difficulties associated

with titanium alloy machining, contributing valuable insights into the effects of dry machining on the material. Dry machining is also regarded as the cleanest approach to machining, as it does not require cutting fluid during the operation. In recent years, there has been an increasing awareness of health and environmental issues, leading to the implementation of new legislations and stricter rules to achieve cleaner production and minimize harmful effects. As a result, it has a reduced impact on environmental degradation due to the absence of cutting fluid application.

The machining setup used for conducting turning experiments is shown in Fig. 1. The ISO 3685 single-point testing standard was used to measure the maximum flank wear (VB max) of 0.6 mm and the average flank wear (*VB*) of 0.3 mm for the tool's useful life [23]. Following each cutting pass, the optical microscope was used to inspect the cutting inserts and determine the flank wear based on the ISO Specification. Equations (1) and (2) were then used to estimate the wear rate (*R*).

$$R = \log\left[VB/l_s\right] = \log\left[VB/1000 t V_c\right] \tag{1}$$

Here, *ls* is the spiral cutting length, *t* is the machining time, and $V_c$ is the cutting speed.

Equation (2) gives the actively engaged cutting time.

$$t = \pi D1/1000 f V c \tag{2}$$

where *D* is the workpiece diameter, *l* is the axial length of the cut, and *f* is the feed rate.

The monitoring of energy consumption during the cutting process was carried out using the method of estimating the difference between the air cut power and the actual cutting power, as outlined in Eqs. (3) and (4). The experimental setup utilizes a Power Analyzer CW 240-F from YOKOGAWA Electric Corporation to measure the cutting power during machining experiments shown in Fig. 1. The power analyzer delivers values for power, current, and voltage through probes attached to the control panel. This methodology has been widely used in previous research studies to measure energy consumption during machining operations [4, 24, 25].

**Table 4** Analysis of variance for wear

| Source | DF | Seq SS | Contribution | Adj SS | Adj MS | F-value | P-value |
|--------|-----|--------|--------------|--------|--------|---------|---------|
| Cutting speed (m/min) | 4 | 0.8498 | 32.79% | 0.8498 | 0.21244 | 11.43 | 0.000 |
| Feed rate (mm/rev) | 3 | 1.1472 | 44.27% | 1.1472 | 0.38241 | 20.58 | 0.000 |
| Error | 32 | 0.5947 | 22.95% | 0.5947 | 0.01859 | | |
| Lack-of-fit | 12 | 0.2379 | 9.18% | 0.2379 | 0.01983 | 1.11 | 0.403 |
| Pure error | 20 | 0.3568 | 13.77% | 0.3568 | 0.01784 | | |
| Total | 39 | 2.5917 | 100.00% | | | | |

**Table 5** Analysis of variance SCE

| Source | DF | Seq SS | Contribution | Adj SS | Adj MS | F-value | P-value |
|---|---|---|---|---|---|---|---|
| Cutting speed (m/min) | 4 | 0.282240 | 87.55% | 0.282240 | 0.070560 | 77.43 | 0.000 |
| Feed rate (mm/rev) | 3 | 0.010990 | 3.41% | 0.010990 | 0.003663 | 4.02 | 0.016 |
| Error | 32 | 0.029160 | 9.04% | 0.029160 | 0.000911 | | |
| Lack-of-fit | 12 | 0.008960 | 2.78% | 0.008960 | 0.000747 | 0.74 | 0.700 |
| Pure error | 20 | 0.020200 | 6.27% | 0.020200 | 0.001010 | | |
| Total | 39 | 0.322390 | 100.00% | | | | |

**Table 6** Cutting conditions selected for SEM/EDX analysis

| Sr. # | Cutting speed (m/min) | Feed (mm/rev) |
|---|---|---|
| 1 | 50 | 0.2 |
| 2 | 52.5 | 0.2 |
| 3 | 55 | 0.2 |
| 4 | 62.5 | 0.2 |
| 5 | 72.5 | 0.2 |
| 6 | 75 | 0.2 |

$$P_{cut} = P_{actual} - P_{air} \tag{3}$$

$$SCE = P_{cut}/MRR \tag{4}$$

The chip compression ratio was also measured for all the samples by determining the chip thickness after the cut ($h_2$) and chip thickness before the cut ($h_1$). In the case of single-point turning, the uncut chip thickness value is the same as the feed rate. The values were then used in Eq. (5) for the compression ratios [26, 27].

$$\text{Compression ratio}, r = \frac{h_2}{h_1} \tag{5}$$

Additional experiments were later carried out to validate and investigate cutting conditions from published data and listed under Sec 3.1. To further investigate the tribological interactions in the regions of interest, cutting conditions were selected based on the published maps for dry machining of Ti6Al4V, traversing the low, moderate, and high tool wear regions. Worn inserts were then examined under optical and electron microscopes for SEM/EDX analysis of transfer between the tool material and the workpiece alloy.

## 3 Results and discussions

The results obtained for tool wear and energy consumption as a result of the full factorial experiments are presented in Table 3. The wear rate ($R$) was calculated based on the maximum wear ($VB_{max}$) measured from a microscope embedded with a digital camera. It can be seen from Fig. 2 that the tool wear rate increases with increasing the cutting speed and feed indicated by the negative value of $R$, the higher the negative value the lower the tool wear. Analysis of the SCE is also important in comparing the energy response of a machine tool. The effect of cutting conditions on the SCE of the machine
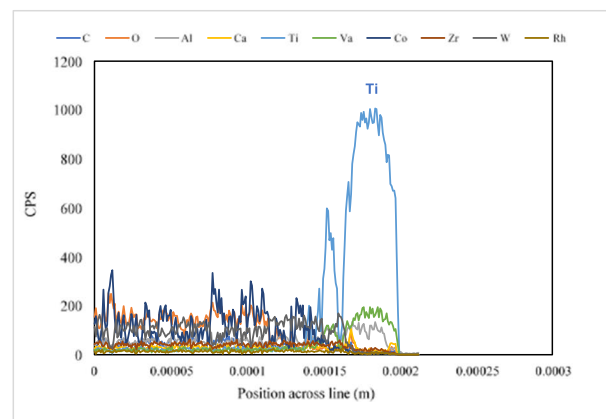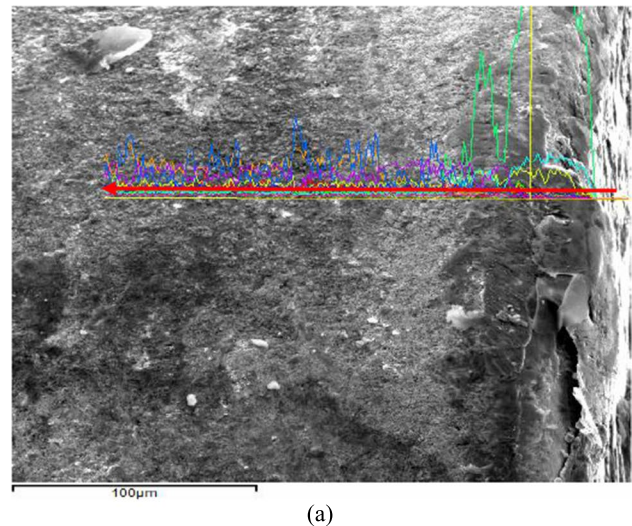


(a)



(b)

**Fig. 6** **a** SEM micrograph showing the elemental mapping performed using line scan analysis. **b** Elemental mapping performed on the used insert with counts per second (CPS) against the position across the line

**Table 7** Wear rate of cutting conditions selected for BUE and line scan analysis

| Sr. # | Cutting speed (m/min) | Feed (mm/rev) | Wear rate | Wear region |
|-------|------------------------|---------------|-----------|-------------|
| 1 | 50 | 0.2 | −6.00 | Low |
| 2 | 52.5 | 0.2 | −5.83 | High |
| 3 | 55 | 0.2 | −5.74 | High |
| 4 | 62.5 | 0.2 | −5.68 | High |
| 5 | 72.5 | 0.2 | −5.67 | High |
| 6 | 75 | 0.2 | −5.99 | Moderate |

tool is shown in Fig. 3. The effect of feed on the SCE is widely reported for aluminum and titanium alloys [28–30]. It can also be argued that an increase in the feed rate leads to higher cutting loads and an improved material removal rate, resulting in lower energy consumption per unit of material removal. This is because, at higher feed rates, the machining mechanics shift towards an effective shearing mechanism rather than a rubbing mechanism, reducing energy consumption [7, 31]. It was observed that the energy consumption is also mainly affected by the increase in the cutting speed as also reported in the literature [32, 33]. The tool wear and energy are further analyzed in the following sections.

Tables 4 and 5 present the analysis of variance (ANOVA) for the data processed using statistical analysis in MINITAB®. The results indicate that the tool wear rate is significantly influenced by both cutting speed (33%) and feed rate (44%). For specific cutting energy (SCE), cutting speed is the most significant factor, contributing to 88% of the variance. These findings are also illustrated using main effect plots, displaying data means and surface plots (Fig. 4). Furthermore, the main effect plot for SCE reveals an increase with the rise in cutting speed and a decrease with an increase in the feed rate. Conversely, for tool wear, an increase is observed with higher cutting speed and feed rate.
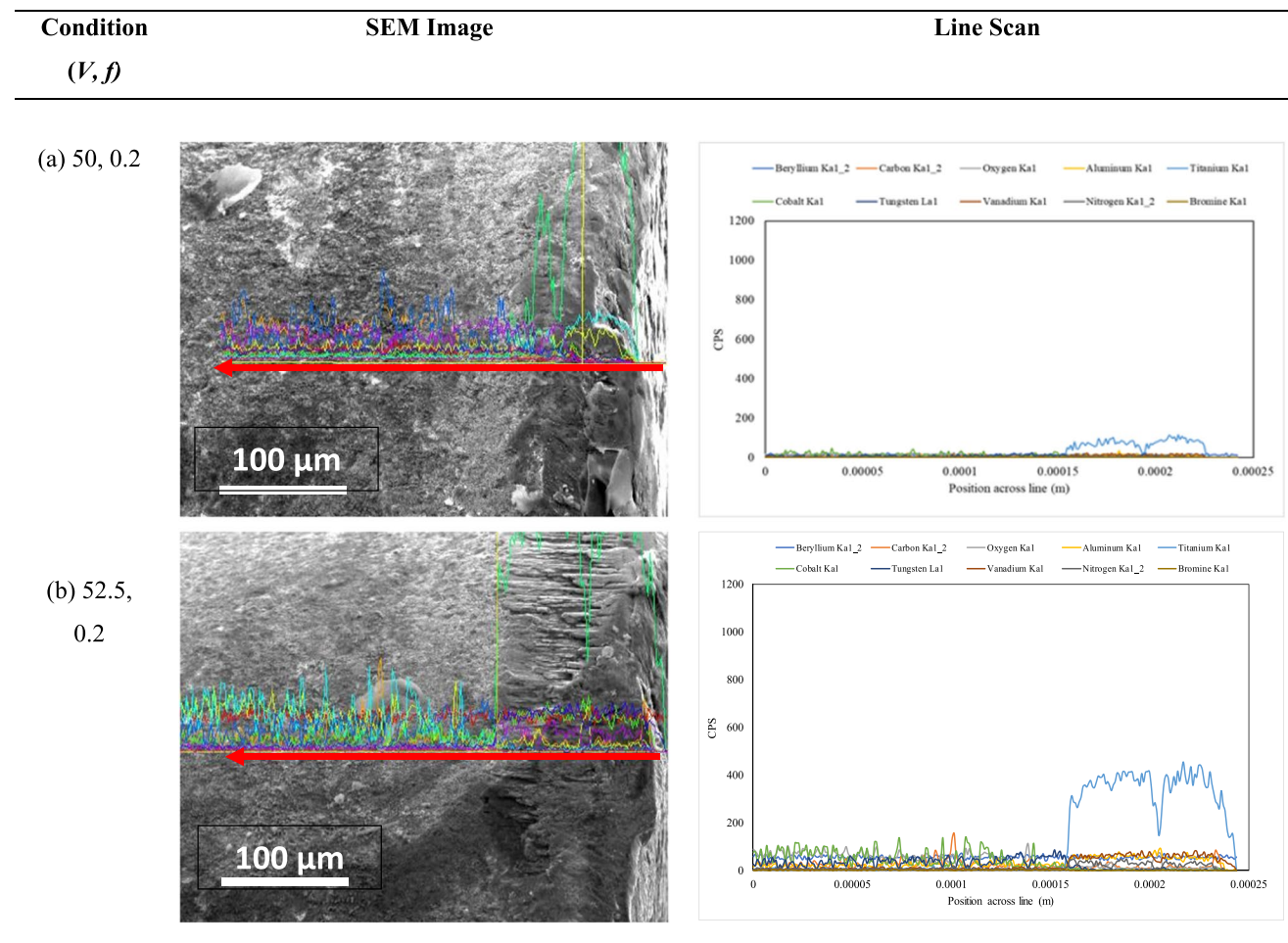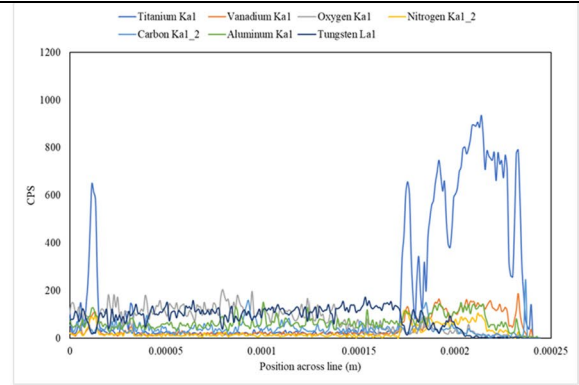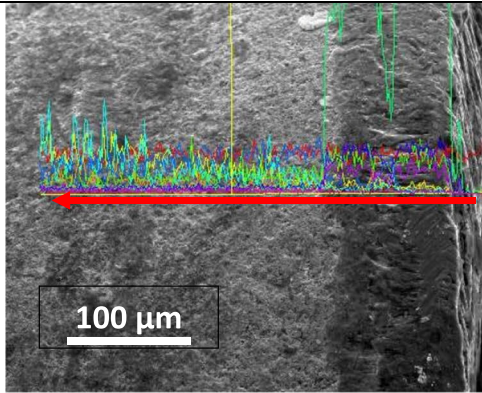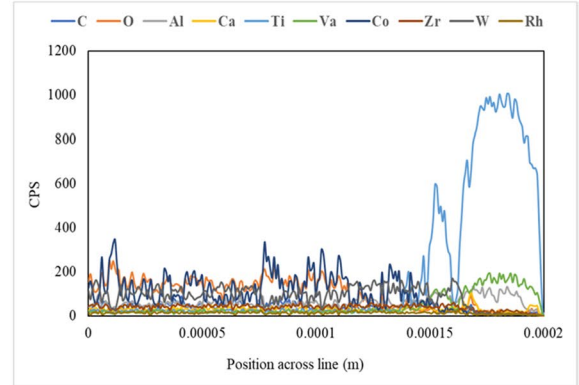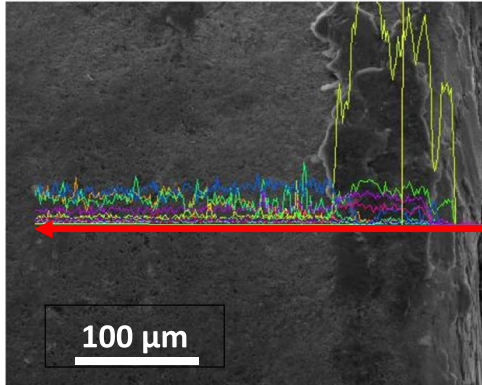


**Fig. 7** Elemental mapping of the cutting edge of used tools obtained from line scan using SEM/EDS
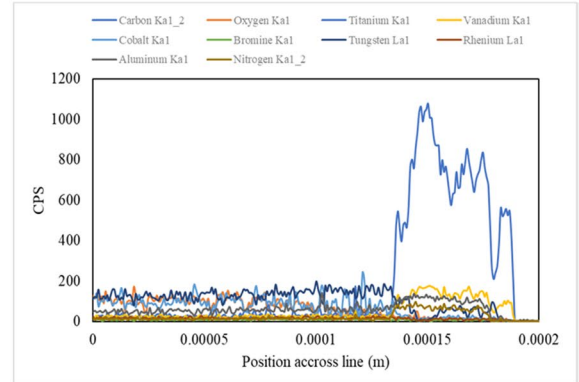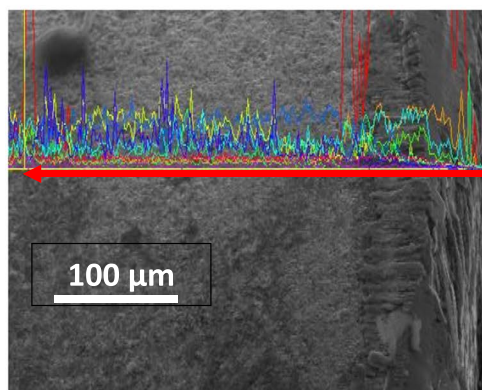
(c) 55, 0.2
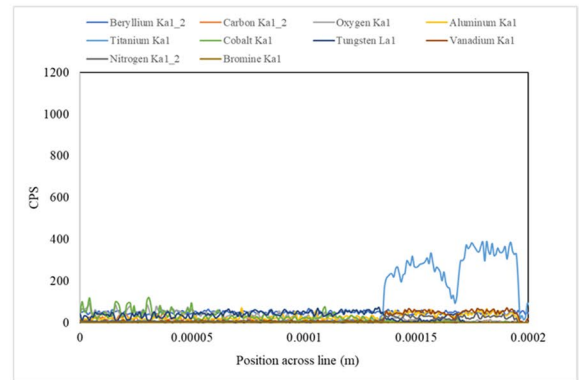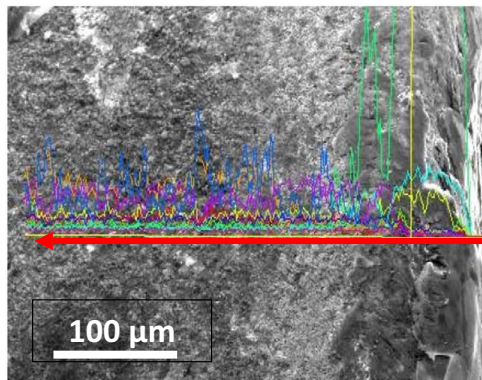


(d) 62.5, 0.2



(e) 72.5, 0.2



(f) 75, 0.2



**Fig. 7** (continued)

**Fig. 8** Increase in adhesion of titanium (**a**) and Vanadium (**b**) on the flank face
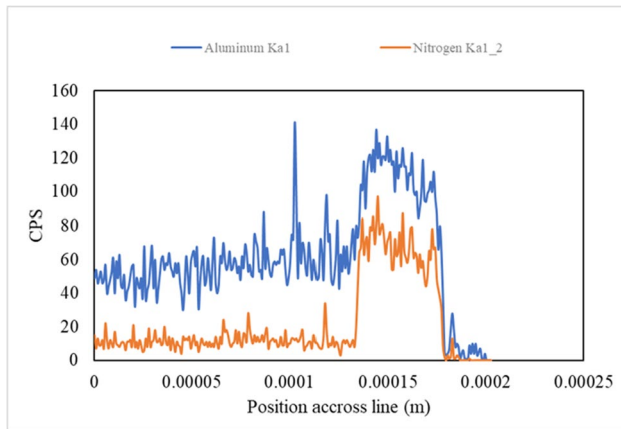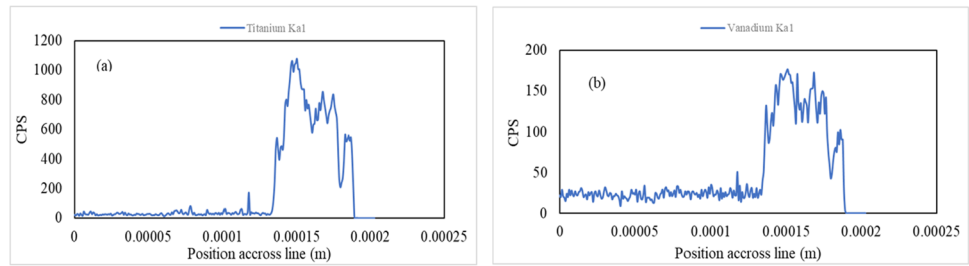




**Fig. 9** Transfer of aluminum and nitrogen from the workpiece to the tool surface

## 3.1 Analysis of tool wear

To further analyze the tool wear, cutting conditions were selected from published data that were reported to have shown low and high tool wear during machining Ti6AL4V, as highlighted by the map in Fig. 5. The experiments in Table 6 were selected from the cutting speeds known for high tool wear, necessitating investigation using SEM/EDX to understand the tool-work interaction at the cutting zone. To cover all three wear zones (low, moderate, and high), the conditions for investigation were selected as shown in the blue highlight. These experiments were performed after each run, and the worn tools were analyzed using SEM to investigate the wear patterns. The results of the tool wear rate estimated from the cutting tests are presented in Table 6. To investigate the tool-chip contact zone, the TESCAN VEGA3 SEM was utilized. Due to the high reactivity of titanium alloys with most tool materials and other elements, elemental mapping on the rake face was performed using energy-dispersive X-ray spectroscopy (EDX). The SEM analysis revealed that titanium adhered to the tool, forming a build-up edge at all cutting conditions.

To examine the worn inserts, a line scan was conducted using the methodologies previously described by researchers [1, 7, 8] (Fig. 6a). The SEM micrograph revealed the adhesion of the material, and Fig. 6b shows the corresponding composition. The graph presents the weight percentage distribution of various elements detected across the flank side and provides a visual representation of the composition in count per second (CPS) against the scanned flank land.

The SEM and elemental mapping results of the used inserts, for cutting conditions as listed in Table 7, are presented in Fig. 7a-f. As previously reported [34, 35], due to the titanium alloy's adhesive tendency and reactive nature with the cutting inserts, a significant amount of workpiece material transfer onto the tool was observed during the EDX analysis of the wear land for all cutting conditions. In all the graphs, the transfer of titanium from the workpiece to the wear zone was noticeable. However, the cutting inserts used for the turning experiments corresponding to the avoidance zone (Fig. 7b-d) exhibited a higher tendency to adhere to the cutting tool edge, resulting in a high tool wear regime. On the other hand, the low wear and moderate wear cutting conditions (left and right

**Fig. 10** Reduction in the percentage of cobalt and tungsten (**a**) and carbon (**b**) from the tool surface
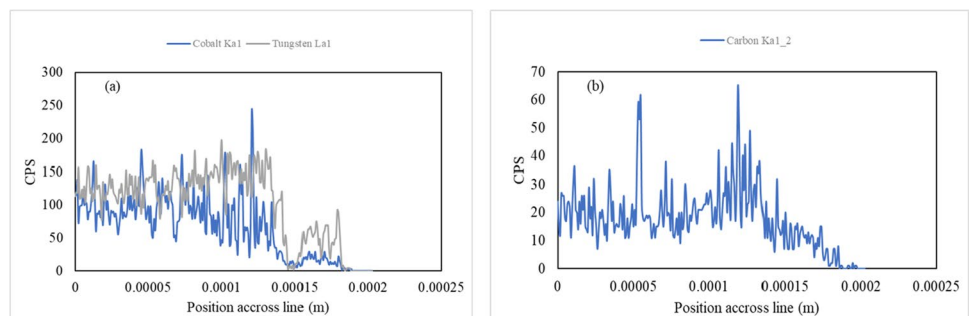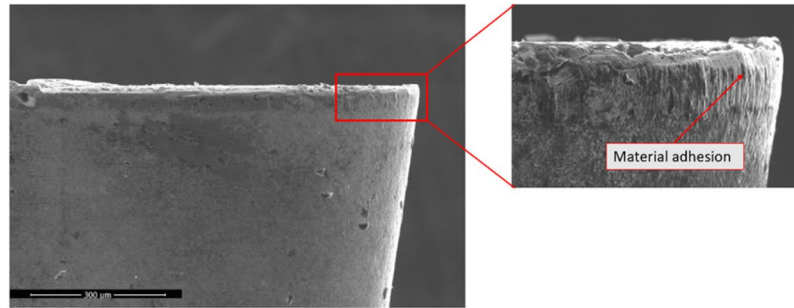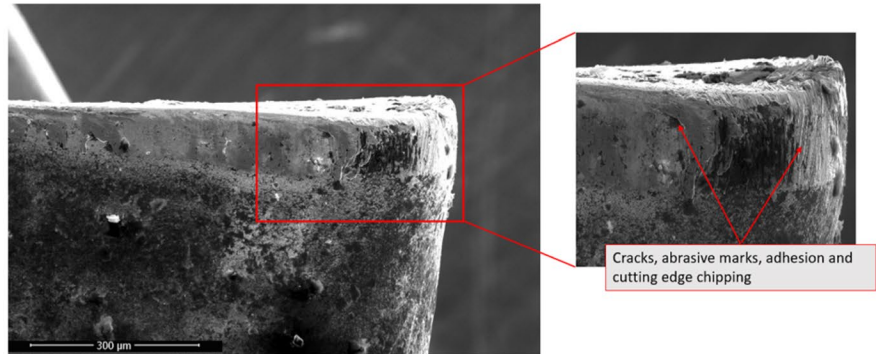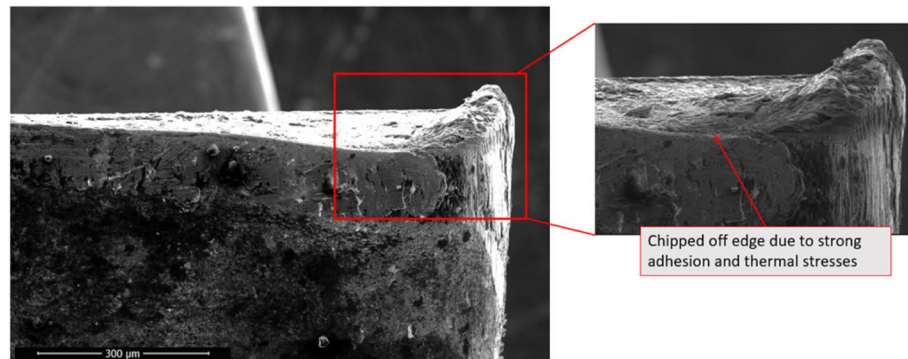
**Fig. 11** SEM images of the tool wear from low (**a**), moderate (**b**, **c**), and high (**d**) wear conditions
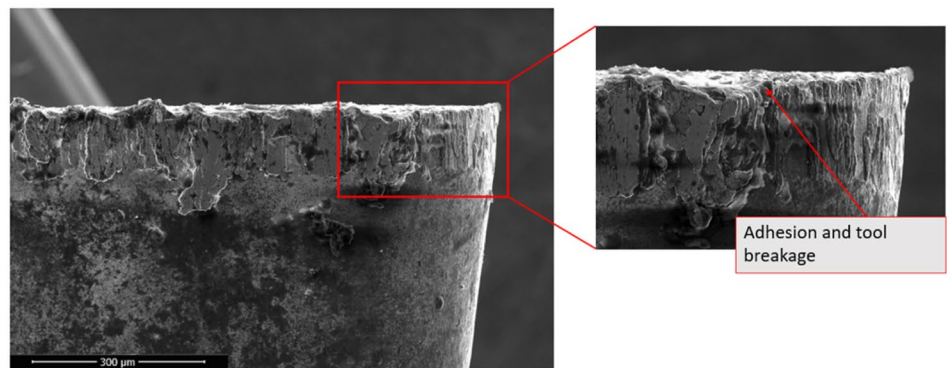


(a)   V= 50 m/min, f = 0.2 mm/rev



(b)   V= 55 m/min, f = 0.2 mm/rev



(c)   V= 62.5 m/min, f = 0.2 mm/rev
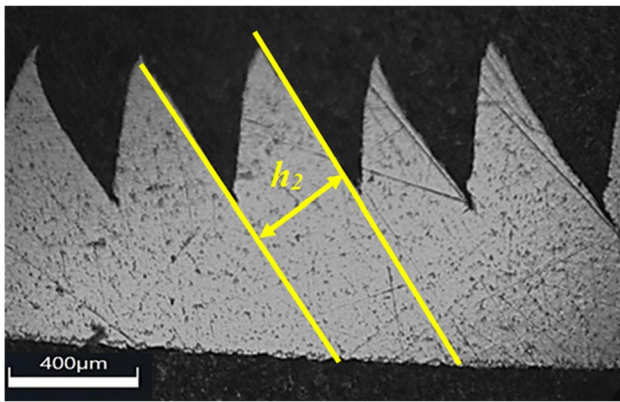


(d)   V= 75 m/min, f = 0.2 mm/rev

**Fig. 12** Chip segment showing after cut chip thickness

**Table 8** Values of SCE and *r* corresponding to the selected zone on the wear map

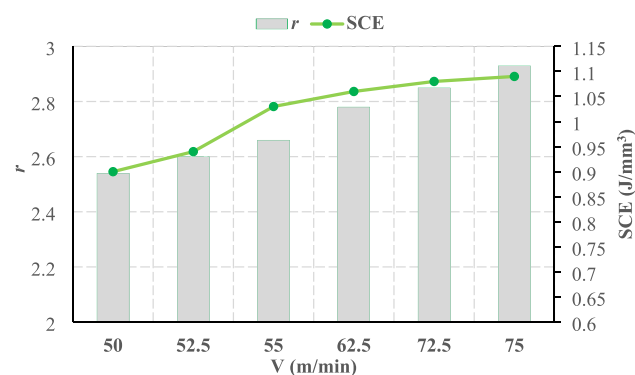| Sr. # | Cutting speed (m/min) | Feed (mm/rev) | SCE | Chip compression ratio |
|---|---|---|---|---|
| 1 | 50 | 0.2 | 0.90 | 2.54 |
| 2 | 52.5 | 0.2 | 0.94 | 2.60 |
| 3 | 55 | 0.2 | 1.03 | 2.66 |
| 4 | 62.5 | 0.2 | 1.06 | 2.78 |
| 5 | 72.5 | 0.2 | 1.08 | 2.81 |
| 6 | 75 | 0.2 | 1.09 | 2.93 |



**Fig. 13** Effect of chip compression on SCE at different cutting speeds

points to the avoidance zone) resulted in the least adhesion, respectively. Thus, the workpiece material adhesion in the avoidance zone caused the high wear of the tools in the cutting speed range of 52.5–72.5 m/min and feed of 0.20 mm/rev on the wear map. This also agrees with the results reported by similar researchers [36, 37].

The investigation of the tribological interactions at the tool-chip region revealed the transfer of various elements between the tool and the workpiece. To investigate this

further, a cutting condition ($V$ = 72.5 m/min and $f$ = 0.2 mm/rev) was selected, and detailed analysis showed an increase in the atomic concentration of titanium and vanadium from the workpiece onto the tool, as demonstrated in Figure 8a, b. Furthermore, an increase in the amount of atmospheric aluminum and nitrogen was observed in the wear region, indicating the formation of TiN or TiAlN, among other elements [16].

Figure 9 shows the increase in the atomic concentration of aluminum and nitrogen. In contrast, the percentage of carbon, tungsten, and cobalt decreased on the tool surface, indicating the transfer of the tool material to the workpiece, as shown in Fig. 10a, b. Line scan tests for all examined inserts revealed that the mass percentage of carbon fell in flank regions, indicating substrate adhesion. Therefore, it can be inferred that the high wear of the cutting tools during titanium machining is due to their reactive nature with the tool material, resulting in diffusion and dissolution that degrade cutting performance and weaken the tool edge [36]. As a result, this phenomenon is the primary source of rapid wear in the avoidance zone.

## 3.2 Wear modes

One of the main problems of tool wear and failures in titanium machining is attributed to the material adhesion on the tool's surface accelerated by the chemical instability and chip material adhesion. This is accelerated by the complex wear phenomenon and the temperature effects at the chip tool interface [15]. In recent studies, important wear mechanisms reported for machining Ti6AL4V alloy include adhesion and abrasion, dissolution and diffusion, attrition, chipping, and plastic deformation [16]. Adhesion of material to the tool's flank and rake surface cause high friction due to direct contact resulting in more severe adhesion and abrasion layer [17].

The SEM images of the cutting condition in the avoidance region were analyzed to identify the wear mechanisms. Figure 11 displays the flank surface of the tool, where low, moderate, and high worn tools were observed, indicating the presence of a complex wear phenomenon at the tool-chip interface. The cutting conditions (avoidance zone) showed severe marks of chip adhesion and high chemical instability, which promoted tool wear at cutting conditions (Fig. 11b, c). Titanium adhered to the tool surface under all conditions, but it was more apparent in the high wear conditions. Many researchers including the current work have reported that materials transfer between the tool and work occurs as a result of elemental diffusion and chemical reaction of the titanium during the machining process, [15, 18]. Additionally, the cutting edge is chipped off, with some abrasive marks present, which has been reported by other researchers for uncoated tools [38]. The uncoated tools'

**Fig. 14** Segmented chips of Ti6Al4V under different cutting conditions



| Cutting Condition (m/min) | | Cutting Condition (m/min) | |
|---|---|---|---|
| V= 50 | | V= 62.5 | |
| V= 52.5 | | V= 72.5 | |
| V= 55 | | V= 75 | |
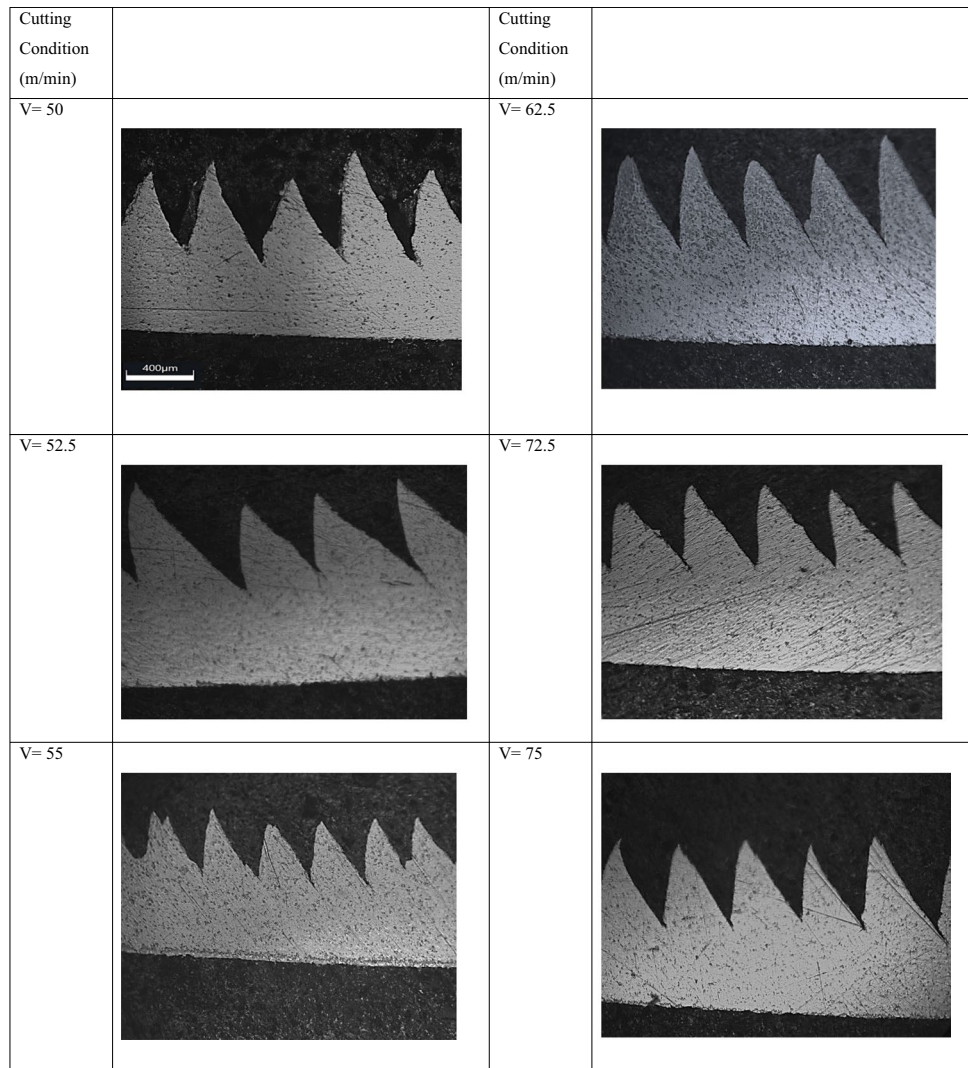
wear is caused by material adhesion-dissolution, poor titanium conductivity, and complex phenomena at the cutting zone, resulting in adhesive wear being the primary cause of high tool wear in the avoidance region [39]. This has also affected the cutting mechanics, forces, and energy during material removal, which will be discussed in the following sections.

### 3.3 Analysis of chip formation and SCE

Chip produced in the machining process was collected and the cross-section of the chip samples after grinding and polishing was also analyzed in optical and SE microscopes. Chip compression ($r$) refers to the deformation of a chip during the cutting process. Therefore, this ratio can be utilized to determine chip generation efficiency, shear angle, pressures, and energy consumption in a cutting cycle [40]. A bigger $r$ number usually corresponds to a narrower shear plane angle, resulting in more energy

consumed throughout the operation. The chip compression ratio was measured using Eq. (5) from the ratio of the chip thickness after the cut ($h_2$) to that of uncut chip thickness ($h_1$) [19], shown in Fig. 12.

Table 8 shows the chip compression ratios and the specific cutting energy consumed during the experimental runs. The specific energy consumption at the tool tip increased with an increase in the cutting speed and accelerated wear. The change in SCE as a result of an increase in chip compression ratio is shown in Fig. 13. Thus, the ratio can also be used as a true representation of the external work and true plastic deformation caused by the tool that represents energy spent in cutting [41]. Moreover, the chip morphologies of the cutting conditions selected showed that shear banding occurred under all the cutting speeds while dry machining Ti6Al4V alloy as shown in Fig. 14. Thus, it can be summarized that the increase in the wear rate in the avoidance zone has also affected the chip geometry, compression ratios, and corresponding SCE consumption during the machining process.

**Fig. 15** Key factors for machinability analysis
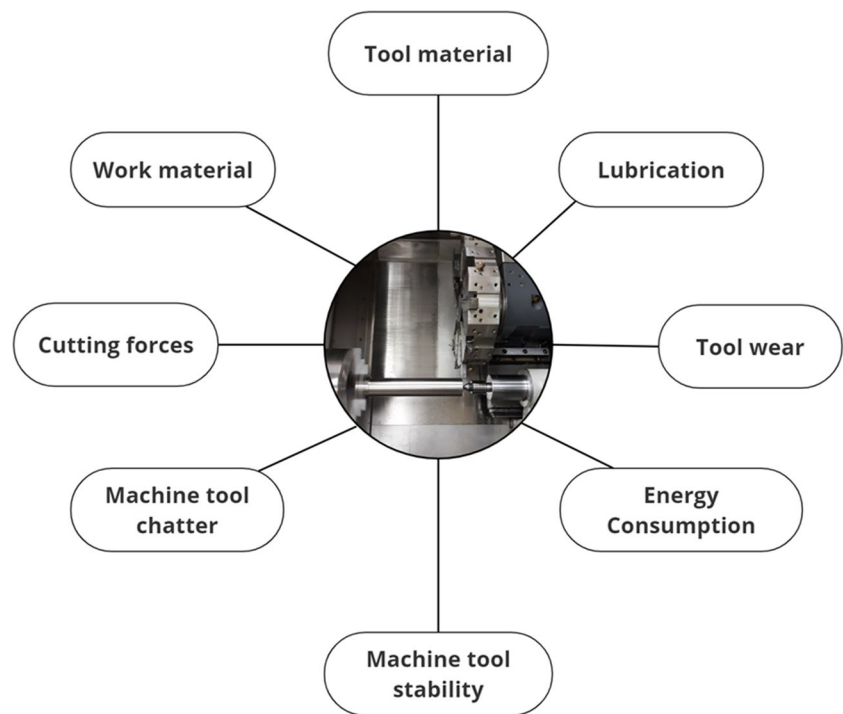


Machine tools and machining process dynamics are crucial for optimizing the manufacturing processes to meet end-user requirements such as precision, cutting performance, and productivity. Many factors can affect a particular machining process; however, during the actual process, the dynamic cutting forces, chatter, machining dynamics, tool wear, and energy consumption are essential in machining studies as highlighted in Fig. 15. Optimal chatter-free conditions can be found for any machining process characterized by stability charts. It has been reported that the chatter and vibration change with the change in the tool wear resulting in cutting instability [42]. The current study has only considered the effect of wear on energy consumption in turning titanium alloy. It is important to mention here that the tool wear and cutting energy are also influenced by dynamic cutting forces, torques, and chatter that vary during the process, impacting the complex phenomenon relating to tool-work interaction, stability, and surface roughness. As a result, tool wear characteristics must be considered in machining and thus further efforts are needed to optimize these diverse responses to improve process efficiency and production quality.

## 4 Conclusions

This research aimed to investigate the energy consumption and wear mechanisms in uncoated tools after turning Ti6AL4V alloy using SEM/EDX and to correlate tool wear with process energy consumption.

- Cutting conditions have a key role in the energy consumption and life of the tool in machining titanium alloys.
- The high wear of cutting tools during machining of titanium-based alloys is due to the reactive nature of titanium with the tool material, leading to the diffusion and dissolution of tool material and degradation of cutting performance.
- The transfer of tool material to the workpiece was confirmed through SEM/EDX analysis, with an increase in the atomic concentration of aluminum and nitrogen and a decrease in the percentage of carbon, tungsten, and cobalt on the tool surface. Line scan tests also revealed substrate adhesion in the flank regions, further supporting the wear mechanism.
- The analysis of the tools with SEM/EDX enabled visualization and distribution of reaction products of the flank wear region occurring at different cutting speeds. By identifying regions of high tool wear rate and examining the material transition between the tool and workpiece, the study shows that avoiding cutting conditions in the high-wear region can lead to cost and energy benefits in machining titanium-based alloys.
- The findings suggest that the high wear rates in the avoidance zone not only affect tool wear but also have an impact on chip morphology and energy consumption during the machining process. The study can also guide the development of suitable tool coatings and lubrication strategies for improving tool life and sustainability in titanium machining.

- The identification of the avoidance zone on the published wear and energy maps can help machinists avoid the cutting conditions corresponding to high-wear regions and achieve cost and energy benefits in machining titanium-based alloys.

**Author contribution** All authors contributed to the study design, analysis, and review.

## Declarations

**Conflict of interests** The authors declare no competing interests.

**Open Access** This article is licensed under a Creative Commons Attribution 4.0 International License, which permits use, sharing, adaptation, distribution and reproduction in any medium or format, as long as you give appropriate credit to the original author(s) and the source, provide a link to the Creative Commons licence, and indicate if changes were made. The images or other third party material in this article are included in the article's Creative Commons licence, unless indicated otherwise in a credit line to the material. If material is not included in the article's Creative Commons licence and your intended use is not permitted by statutory regulation or exceeds the permitted use, you will need to obtain permission directly from the copyright holder. To view a copy of this licence, visit http://creativecommons.org/licenses/by/4.0/.

## References

1. Younas M, Jaffery SHI, Khan M, Khan MA, Ahmad R, Mubashar A et al (2019) Multi-objective optimization for sustainable turning Ti6Al4V alloy using grey relational analysis (GRA) based on analytic hierarchy process (AHP). Int J Adv Manuf Technol 105:1175–88

2. Ezugwu EO, Bonney J, Yamane Y (2003) An overview of the machinability of aeroengine alloys. J Mater Process Technol 134(2):233–253

3. Stephenson DA, Agapiou JS (2023) Metal cutting theory and practice. CRC press

4. Khan MA, Jaffery SHI, Khan M, Younas M, Butt SI, Ahmad R et al (2020) Multi-objective optimization of turning titanium-based alloy Ti-6Al-4V under dry, wet, and cryogenic conditions using gray relational analysis (GRA). Int J Adv Manuf Technol 106:3897–911

5. Cozzi L, Gould T, Bouckart S, Crow D, Kim TY, McGlade C, Olejarnik P, Wanner B, Wetzel D (2020) World energy outlook 2020. International Energy Agency, Paris, France

6. BEIS, Digest of UK Energy Statistics (DUKES) (2021) Department for business, energy and industrial strategy. London, UK

7. Beis (1994). Energy Consumption in the UK (ECUK) 1970 to 2021 million tonnes of oil equivalent Industry Transport Services Domestic

8. Deif AM (2011) A system model for green manufacturing. J Clean Prod 19:1553–9

9. Goindi G, production PSJ of cleaner, (2017 undefined) Dry machining: a step towards sustainable machining–challenges and future directions. Elsevier [Internet] [cited 2023 Apr 8]; Available from: https://www.sciencedirect.com/science/article/pii/S0959652617316918?casa_token=J8dLpiJy4EoAAAAA:adLPApGGfhDo0dSdDU-E7mdmp2r7QsqkpFTw7066hmZXg0O0QMjfUNi7XgWuVjUq4KzH8wEB. Accessed 8 Apr 2023

10. Jianxin D, Yousheng L, Wenlong S (2008) Diffusion wear in dry cutting of Ti–6Al–4V with WC/Co carbide tools. Wear 265:1776–83

11. Younas M, Husain Imran Jaffery S, Khan M, Ahmad R, Ali L, Khan Z et al (2019) Tool wear progression and its effect on energy consumption in turning of titanium alloy (Ti-6Al-4V). Mech Sci 10:373–82

12. Bermingham MJ, Kirsch J, Sun S, Palanisamy S, Dargusch MS (2011) New observations on tool life, cutting forces and chip morphology in cryogenic machining Ti-6Al-4V. Int J Mach Tools Manuf 51:500–11

13. Arrazola PJ, Garay A, Iriarte LM, Armendia M, Marya S, Le Maître F (2009) Machinability of titanium alloys (Ti6Al4V and Ti555.3). J Mater Process Technol 209:2223–30

14. Gu J, Barber G, Tung S, Wear RG, (1999 undefined) Tool life and wear mechanism of uncoated and coated milling inserts. Elsevier [Internet] [cited 2023 Apr 8]; Available from: https://www.sciencedirect.com/science/article/pii/S0043164899000745?casa_token=Nt-YakYSK1IAAAAA:YJii-89JY2Cg-uF7yG5Qg_sNARudqqzYSSmDWUouJL3boGwfMo3I2X1axPYxl6bzaamXgGk. Accessed 8 Apr 2023

15. Chou Y, Wear CE, (1997 undefined). Tool wear mechanism in continuous cutting of hardened tool steels. Elsevier [Internet] [cited 2023 Apr 8]; Available from: https://www.sciencedirect.com/science/article/pii/S0043164897001397

16. Jaffery SHI, Mativenga PT (2012) Wear mechanisms analysis for turning Ti-6Al-4V-towards the development of suitable tool coatings. Int J Adv Manuf Technol 58:479–93

17. Rahman Rashid RA, Palanisamy S, Sun S, Dargusch MS. (2016) Tool wear mechanisms involved in crater formation on uncoated carbide tool when machining Ti6Al4V alloy. International Journal of Advanced Manufacturing Technology [Internet] [cited 2023 Apr 8];83:1457–65. https://doi.org/10.1007/s00170-015-7668-z

18. Saketi S, Odelros S, Östby J, Olsson M (2019) Experimental study of wear mechanisms of cemented carbide in the turning of Ti6Al4V. Materials 12:2822 Available from: https://www.mdpi.com/1996-1944/12/17/2822/htm

19. Younas M, Jaffery SHI, Khan A, Khan M (2021) Development and analysis of tool wear and energy consumption maps for turning of titanium alloy (Ti6Al4V). J Manuf Process 62:613–22

20. Ahmada R (2019) Process parameters and its effect on surface roughness during turning Ti6Al4V alloy. In: Advances in Manufacturing Technology XXXIII: Proceedings of the 17th International Conference on Manufacturing Research, incorporating the 34th National Conference on Manufacturing Research, 10-12 September 2019. Queen's University, Belfast, vol 9. IOS Press, p 303

21. Venkata Rao K (2019) Power consumption optimization strategy in micro ball-end milling of D2 steel via TLBO coupled with 3D FEM simulation. Measurement 132:68–78 https://www.sciencedirect.com/science/article/pii/S0263224118308789

22. Rao KV, Kumar YP, Singh VK, Raju LS, Ranganayakulu J (2021) Vibration-based tool condition monitoring in milling of Ti-6Al-4V using an optimization model of GM(1, N) and SVM. Int J Adv Manuf Technol 115:1931–41. https://doi.org/10.1007/s00170-021-07280-3. Available from

23. ISO I 3685 (1993) Tool-life testing with single-point turning tools. International Organization for Standardization (ISO), Geneva, Switzerland

24. Jaffery SHI, Younas M, Khan M, Ali L (2020) Energy consumption analysis in turning Ti-6Al-4V alloy. In: 2020 IEEE 11th International Conference on Mechanical and Intelligent Manufacturing Technologies (ICMIMT). IEEE, pp 18–21

25. Khan MA, Jaffery SHI, Khan M, Younas M, Butt SI, Ahmad R et al (2019) Statistical analysis of energy consumption, tool wear and surface roughness in machining of titanium alloy (Ti-6Al-4V) under dry, wet and cryogenic conditions. Mech Sci 10:561–73

26. Astakhov VP, Shvets S (2004) The assessment of plastic deformation in metal cutting. J Mater Process Technol 146:193–202

27. Iqbal SA, Mativenga PT, Sheikh MA (2007) Characterization of machining of AISI 1045 steel over a wide range of cutting speeds. Part 1: Investigation of contact phenomena. Proc IME B J Eng Manufact 221(5):909–916

28. Warsi SS, Jaffery SHI, Ahmad R, Khan M, Ali L, Agha MH et al (2017) Development of energy consumption map for orthogonal machining of Al 6061–T6 alloy. Proc Inst Mech Eng B J Eng Manuf 232:2510–22. https://doi.org/10.1177/0954405417703424

29. Khan M, Warsi SS, Jaffery SH, Ahmad R, Younas M (2019) Analysis of energy consumption in orthogonal machining of Al 6061-T6 alloy. In: Advances in Manufacturing Technology XXXIII: Proceedings of the 17th International Conference on Manufacturing Research, incorporating the 34th National Conference on Manufacturing Research, 10–12 September 2019. Queen's University, Belfast, vol 9. IOS Press, p 327

30. Khan MA, Jaffery SHI, Khan M (2023) Assessment of sustainability of machining Ti-6Al-4V under cryogenic condition using energy map approach. Eng Sci Technol Int J 41:101357 https://www.sciencedirect.com/science/article/pii/S2215098623000344

31. Balogun VA, Mativenga PT (2014) Impact of un-deformed chip thickness on specific energy in mechanical machining processes. J Clean Prod 69:260–8 (https://www.sciencedirect.com/science/article/pii/S0959652614000493)

32. Khan MA, Jaffery SHI, Khan M, Younas M, Butt SI, Ahmad R et al (2020) Multi-objective optimization of turning titanium-based alloy Ti-6Al-4V under dry, wet, and cryogenic conditions using gray relational analysis (GRA). Int J Adv Manuf Technol 106:3897–911

33. Behrendt T, Zein A, Min S (2012) Development of an energy consumption monitoring procedure for machine tools. CIRP Ann Manuf Technol 61:43–6

34. Pramanik A, Littlefair G (2015) Machining of titanium alloy (Ti-6Al-4V)—theory to application. Mach Sci Technol 19(1):1–49

35. Zawada-Tomkiewicz A, Żurawski Ł, Tomkiewicz D, Szafraniec F. (2021) Sustainability and tool wear of titanium alloy thread cutting in dry and cryogenic conditions. Int J Adv Manuf Technol [Internet] [cited 2023 Apr 10];114:2767–81. Available from: https://doi.org/10.1007/s00170-021-07034-1

36. Jamil M, He N, Gupta MK, Zhao W, Khan AM (2022) Tool wear mechanisms and its influence on machining tribology of face milled titanium alloy under sustainable hybrid lubri-cooling. Tribol Int 170:107497

37. Semones PT, Bedekar VM, Bhat DG, Batzer SA (2004) Tool/workpiece chemical transfer on standard WC-Co tool inserts in turning on Ti-6Al-4V. J Mech Behav Mater 15(1–2):1–2

38. Jawaid A, Che-Haron CH, Abdullah A (1999) Tool wear characteristics in turning of titanium alloy Ti-6246. J Mater Process Technol 92–93:329–34 https://www.sciencedirect.com/science/article/pii/S0924013699002460

39. Hartung PD, Kramer BM, Von Turkovich BF (1982) Tool wear in titanium machining. CIRP Annals 31:75–80

40. Groover MP (2020) Fundamentals of modern manufacturing: materials, processes, and systems. John Wiley & Sons

41. Astakhov VP, Shvets S. (2004) The assessment of plastic deformation in metal cutting. J Mater Process Technol [Internet] [cited 2023 Apr 25];146:193–202. Available from: https://linkinghub.elsevier.com/retrieve/pii/S0924013603009981

42. (2008) Machining dynamics: theory, applications and practices, London: Springer